Journal of Biomolecular NMR, **11:** 423–435, 1998.
KLUWER/ESCOM

^{13}C shieldings, ^{18}O isotope effects on ^{13}C shieldings, and ^{57}Fe-^{13}C spin couplings of the Fe-C-O unit in superstructured hemoprotein models: Comparison with hemoproteins, C-O vibrational frequencies, and X-ray structural data

Charalampos G. Kalodimos[a], Ioannis P. Gerothanassis[a,*], Anastasios Troganis[b], Bernard Loock[c] and Michel Momenteau[c,†]

[a]*Department of Chemistry, Section of Organic Chemistry and Biochemistry, University of Ioannina, GR-45110 Ionnina, Greece;* [b]*NMR Center, University of Ioannina, GR-45110 Ionnina, Greece;* [c]*Institut Curie, Section de Recherche, URA 1387 CNRS, Centre Universitaire, F-91405 Orsay, France*

Received 22 October 1997; Accepted 24 December 1997

Key words: ^{13}C shieldings, hemoproteins, isotope effects, model compounds

Abstract

^{13}C NMR spectra of several carbon monoxide (99.7% ^{13}C and 11.8% ^{18}O enriched) hemoprotein models with varying polar and steric effects of the distal organic superstructure and constraints of the proximal side are reported. This enables the ^{57}Fe-^{13}C(O) coupling constants ($^{1}J_{^{57}Fe-^{13}C}$), ^{13}C shieldings ($\delta(^{13}C)$), and ^{18}O isotope effects on ^{13}C shieldings ($^{1}\Delta^{13}C(^{18}O/^{16}O)$) to be measured and hence comparisons with hemoproteins, C-O vibrational frequencies and X-ray structural data to be made. Negative polar interactions in the binding pocket and inhibition of Fe→CO back-donation or positive distal polar interactions with amide NH groups appear to have little direct effect on $^{1}J_{^{57}Fe-^{13}C}$ couplings. Similarly, the axial hindered base 1,2-dimethylimidazole has a minor effect on the $^{1}J_{^{57}Fe-^{13}C}$ values despite higher rates of CO desorption being observed for such complexes. On the contrary, ^{13}C shieldings vary widely and an excellent correlation was found between the infrared C-O vibrational frequencies (ν(C-O)) and ^{13}C shieldings and a reasonable correlation with ^{18}O isotope effects on ^{13}C shieldings. This suggests that $\delta(^{13}C)$, ν(C-O) and $^{1}\Delta^{13}C(^{18}O/^{16}O)$ are accurate monitors of the multiple mechanisms by which steric and electronic interactions are released in superstructured heme model compounds. The ^{13}C shieldings of heme models cover a 4.0 ppm range which is extended to 7.0 ppm when several HbCO and MbCO species at different pH values are included. The latter were found to obey a similar linear $\delta(^{13}C)$ versus ν(C-O) relationship, which proves that both heme models and heme proteins are homogeneous from the structural and electronic viewpoint. Our results suggest that ν(C-O), $\delta(^{13}C)$ and $^{1}\Delta^{13}C(^{18}O/^{16}O)$ measurements reflect similar interaction which is primarily the modulation of π back-bonding from the Fe d_π to the CO π^* orbital by the distal pocket polar interactions. The lack of correlation between $^{1}\Delta^{13}C(^{18}O/^{16}O)$ and crystallographic CO bond lengths (r(C-O)) reflects significant uncertainties in the X-ray determination of the carbon and oxygen positions.

Introduction

The reversible binding of dioxygen and carbon monoxide has played a central role in studies of heme protein structure and function (Dickerson and Geis, 1983; Perutz et al., 1987) and, consequently, the mechanism of the control of the electronic structure and properties of the heme binding site by the protein globule is one of the central problems in modern biochemistry and biophysics (Springer et al., 1994). As a result, numerous encumbered iron(II) porphyrin models, which lack a macromolecular peptide backbone but contain functional groups involved in

* To whom correspondence should be addressed.
† Deceased.

biological processes, have been synthesized in an effort to elucidate the structural details of small ligand binding (Momenteau, 1986; Jameson and Ibers, 1994; Momenteau and Reed, 1994). There has been much discussion on the mechanistic basis of the variation of affinity values of dioxygen and carbon monoxide in heme proteins and model compounds. This has focused on the nature of the axial ligand, distal steric effects, distal polar effects and the enforced doming and ruffling of the porphyrin skeleton (Gerothanassis, 1994; Ray et al., 1994; Tetreau et al., 1994).

It is usually assumed that the Fe-C-O unit prefers a linear geometry, in order to maximize Fe $d_\pi \rightarrow$CO π^* back-bonding, while the FeO_2 unit is strongly bent. Initial attention focused on this bent versus linear dichotomy and on the possibility that the CO binding is inhibited by steric interactions that impede a linear geometry (Collman et al., 1976, 1983b). Indeed, this has become a classic example of the relation between structure and function in proteins (Stryer, 1988). More recently, emphasis has been given to polar interactions in the binding pocket (Oldfield et al., 1991; Park et al., 1991; Ray et al., 1994). Li and Spiro (1988) have interpreted an inverse correlation between ν(C-O) and ν(Fe-C) in terms of back-bond donation from the iron atom. Oldfield et al. (1991) and Kushkuley and Stavrov (1997) emphasized the role of electrostatic influences on isotropic chemical shifts, quadrupole coupling constants and vibrational frequencies in CO-heme proteins. They suggested that the electrical polarization and back-bonding concepts can provide a plausible molecular interpretation of both NMR and IR data of hemoproteins.

One-bond ^{57}Fe-^{13}C coupling constants ($^1J_{^{57}Fe-^{13}C}$), ^{13}C shieldings ($\delta(^{13}C)$), and ^{18}O isotope effects on ^{13}C shielding ($^1\Delta^{13}C(^{18}O/^{16}O)$) can be considered as obvious candidates which might provide a more complete analysis of the nature of Fe-CO bonding. There have been, to date, only two ^{57}Fe-^{13}C coupling constant studies of heme proteins and model compounds (La Mar et al., 1978; Collman et al., 1983a). The ^{13}C shieldings of CO in heme proteins were shown to be linearly related to the weighted averages of the multiple CO vibrational frequencies, demonstrating that $\delta(^{13}C)$ can provide important information on ligand binding hemoproteins (Potter et al., 1990). ^{18}O isotope effects on ^{13}C shielding are limited to the case of free ^{13}CO in $CDCl_3$ solution (Wasylishen et al., 1985).

In this paper, we report ^{13}C shieldings, the observation via ^{13}C NMR of ^{57}Fe-^{13}C coupling constants, and ^{18}O isotope effects on ^{13}C shielding on a number of hemoprotein model compounds (Figure 1). Due to a knowledge of six high-resolution single-crystal X-ray structural data of six-coordinated iron porphyrins with CO, the object of this work was to identify any changes in the ^{57}Fe-^{13}C coupling constants, ^{13}C shieldings and ^{18}O isotope effects on ^{13}C shieldings of bound ^{13}CO as a function of polar and steric effects of the distal organic superstructure and constraints of the proximal side. Also, it was hoped that these NMR measurements might lead to a possible correlation with NMR data of heme proteins, vibrational frequencies and geometric information (e.g. the Fe-C-O bond angle and C-O bond length derived from X-ray diffraction measurements).

Materials and methods

Sample preparation

The iron(III)-porphyrin-superstructure complexes in the chloride form were synthesized and characterized by the methods described previously (Almog et al., 1975; Collman et al., 1983a; Momenteau et al., 1987; El-Kasmi et al., 1993). The complexes were treated in dichloromethane solution. After deoxygenation by flushing with pure argon, the sample was reduced to the iron(II) form using aqueous sodium dithionite solution. After separation of the two phases, the organic layer of the reduced compound was transferred under argon into a second vessel containing an excess of either 1-methylimidazole or 1,2-dimethylimidazole. The resulting powder obtained after removal of the aqueous phase and subsequent evaporation of the organic solvent was then loaded into a glass ampule, connected to a vacuum pump, and evacuated at room temperature for 3 h at a pressure of 10^{-4} torr. The sample was dissolved in deuterated dichloromethane and transferred under argon into the NMR tube via a stainless steel tube. ^{13}CO (99.7% enriched in ^{13}C

Abbreviations: Hb, hemoglobin; Mb, myoglobin; 1-MeIm, 1-methylimidazole; 1,2-diMeIm, 1,2-dimethylimidazole; **A**, α-5,15-[2,2′-(dodecanediamido)diphenyl]-α,α-10,20-bis(*o*-pivaloylamidophenyl)porphyrin; **B**, α-5,15-[2,2′-(decanediamido)diphenyl]-α,α-10,20-bis(*o*-pivaloylamidophenyl)porphyrin; **C**, α-5,15-[2,2′-(octanediamido)diphenyl]-α,α-10,20-bis(*o*-pivaloylamidophenyl)porphyrin; **D**, 5,10,15,20-(α,α,α,α)-(*o*-pivaloylamidophenyl)porphyrin; **E**, 5,10,15-(1,3,5-benzenetriacetyl)-tris(α,α,α-*o*-aminophenyl)-20-(α-*o*-pivaloylamidophenyl) porphyrin; **F**, α-5,15-[2,2′-(dodecanediamido)diphenyl]: β-10,20-{2,2′-(5-imidazol-1-ylnonane-1,9-diamido)diphenyl}porphyrin; **G**, 5,10,15,20-[pyrromellitoyl(tetrakis-*o*-oxyethoxyphenyl]porphyrin; **H**, 5,10,15,20-[pyrromellitoyl(tetrakis-*o*-oxypropoxyphenyl]porphyrin; **I**, 8, 18-bis-(methylpropoxyl)-3,7,13,17-tetramethyl-2,12-(tetradecamethylene)porphyrin.

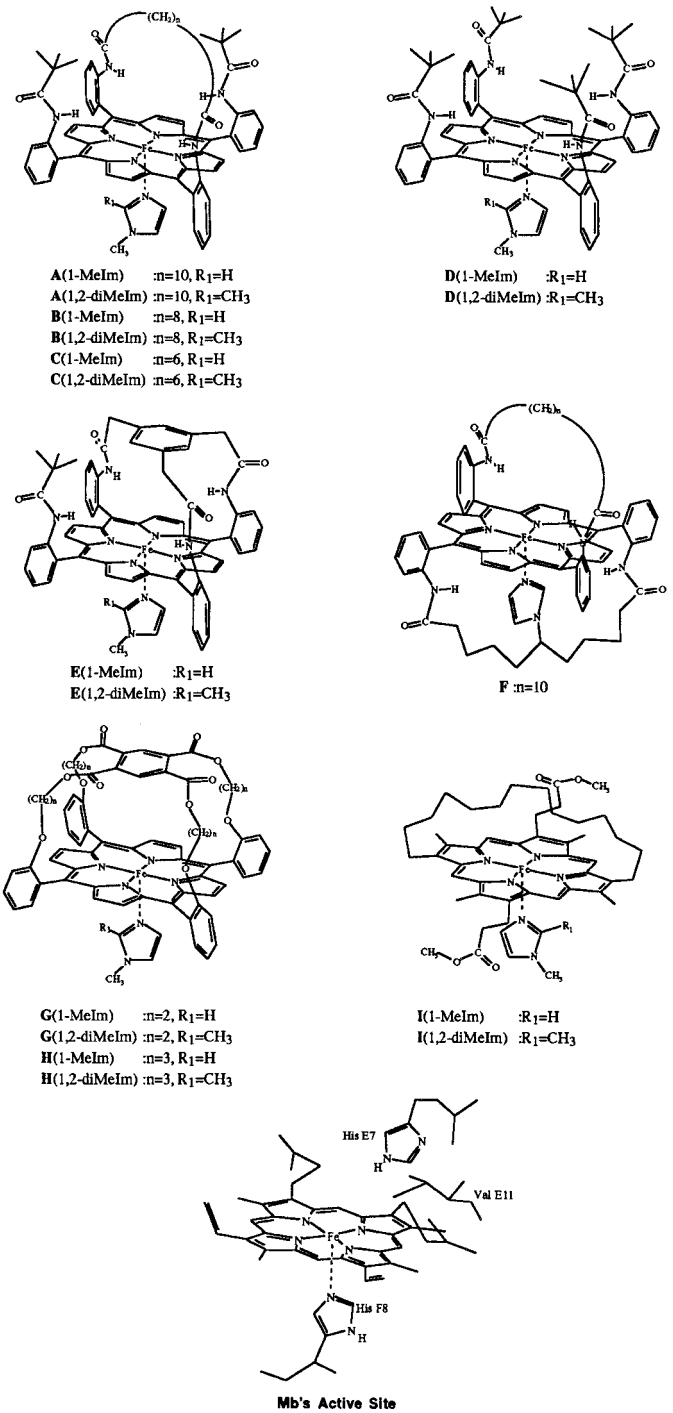

Figure 1. Schematic structures of the heme model compounds studied in this work; the active site of Mb is also included for comparison.

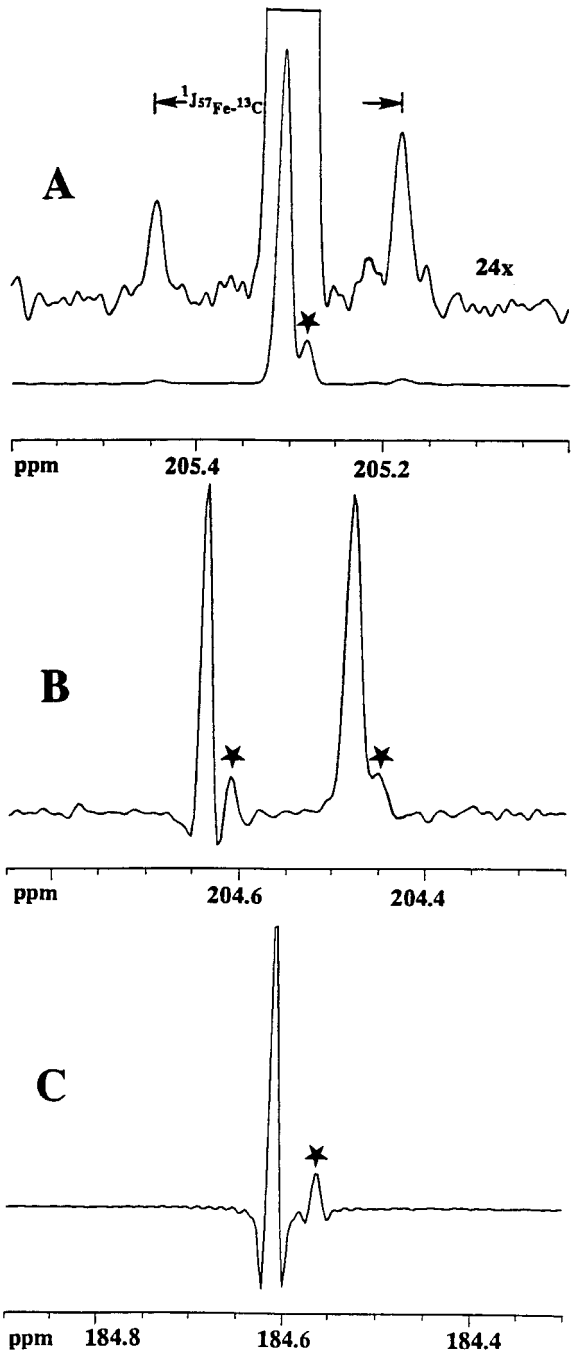

Figure 2. ^{13}C NMR spectra of the ^{13}CO complexes (99.7% enriched in ^{13}C and 11.9% in ^{18}O) of the heme models: (A) **B**(1-MeIm) and (B) **E**(1,2-diMeIm), saturated solution in CD_2Cl_2, at 273 K using a Bruker AMX-400 instrument, $T_{acq} \sim 0.8$ s, number of scans 5000, after resolution enhancement by a Gaussian-exponential function. (C) The ^{13}C NMR spectrum of free ^{13}CO in solution. The arrows denote the $^1J_{^{57}Fe-^{13}C}$ coupling constant. The asterisks denote the ^{18}O isotopically shifted ^{13}C resonances.

and 11.9% in ^{18}O; Euriso-top, group CEA (Saclay, France)) under atmospheric pressure was then introduced to the sample to form the carbonylated derivative and the NMR tube was sealed under a pressure of ~1 atm.

NMR spectra

^{13}C NMR spectra were obtained at 100.62 MHz with a Brüker AMX-400 instrument equipped with a high-resolution probe (5 mm sample tubes). The chemical shifts were determined relative to the resonance position of the solvent ($CD_2Cl_2 \sim 53.8$ ppm). Solvent suppression was achieved by selective irradiation. Overlapping resonances were resolution enhanced by multiplication of the free-induction decay with a Gaussian-exponential function. This function has the form $\exp(\alpha t - bt^2)$, where α (>0) and b (>0) are adjustable parameters.

Results and discussion

Effects of distal site polarity and central steric hindrance (Fe-C-O bond angle) on $^1J_{^{57}Fe-^{13}C}$, $\delta(^{13}C)$ and $^1\Delta^{13}C(^{18}O/^{16}O)$

Figure 2A shows a typical ^{13}C spectrum of the ^{13}CO complex of the 'hybrid' model **B**(1-MeIm). The NMR spectrum consists of a central peak due to the ^{56}Fe-^{13}C moiety and two satellites due to the one-bond ^{57}Fe-^{13}C coupling constant. The relative integral of the center peak compared to that of the two satellites agrees well with the expected one for the natural abundance of 2.2% of the ^{57}Fe isotope. The results of analyzing the isotropic chemical shifts ($\delta(^{13}C)$) and $^1J_{^{57}Fe-^{13}C}$ on all the complexes studied are shown in Table 1. It is found that there is normally no difference in isotropic chemical shifts and one-bond ^{57}Fe-^{13}C couplings at 298 and 273 K.

The ^{13}C-labelled carbon monoxide from commercial sources normally has a considerable enrichment in ^{18}O content, which makes it possible to obtain information on ^{18}O isotope shifts of the same sample. Figure 2 shows typical ^{13}C NMR spectra of the ^{13}CO (99.7% enriched in ^{13}C and 11.9% in ^{18}O) complexes with the heme model compounds **B**(1-MeIm) and **E**(1,2-diMeIm). The asterisks denote the ^{18}O isotopically shifted ^{13}C resonances. From Table 1 it is evident that while the one-bond $^1J_{^{57}Fe-^{13}C}$ coupling constants are practically independent of the nature of both the axial ligand and distal protecting chain, the

Table 1. ^{13}C shieldings ($\delta(^{13}C)$), ^{57}Fe-^{13}C spin couplings ($^{1}J_{^{57}Fe-^{13}C}$), ^{18}O isotope shifts on ^{13}C shielding ($^{1}\Delta^{13}C(^{18/16}O)$), C-O vibrational frequencies (ν(C-O)), and shielding anisotropies (η) of the Fe-C-O unit in the superstructured hemoprotein models of Figure 1

Compound	$\delta(^{13}C)$ (ppm)	$^{1}J_{^{57}Fe-^{13}C}$ (Hz)	$^{1}\Delta^{13}C(^{18/16}O)$ (ppb)	ν(C-O) (cm^{-1})	η[a]
A(1-MeIm)	205.0	26.8	27.0	1958[b]	0.00
A(1,2-diMeIm)	205.6	28.0			0.11
B(1-MeIm)	205.3	27.6	26.5	1952[b]	
B(1,2-diMeIm)	205.6	27.6			
C(1-MeIm)	206.0	26.8	26.0	1948[b]	0.07
C(1,2-diMeIm)	206.2	27.2			0.10
D(1-MeIm)	204.7	27.5	29.8	1969[c]	0.07
D(1,2-diMeIm)	205.0	26.3	27.0	1962[c]	
E(1-MeIm)	204.6	27.4	28.0	1964[d]	0.18
E(1,2-diMeIm)	204.7[e]	26.0[e]	26.6[e]		
	204.6[f]	25.0[f]	27.6[f]		0.15
F[g]	203.9	28.2	29.7	1971[b]	
	204.4	27.2	28.9		
G(1-MeIm)	202.1	27.2	31.5	2002[h]	0.12
G(1,2-diMeIm)	202.2	26.4		1999[h]	0.16
H(1-MeIm)	203.0	27.2	32.0	1979[h]	
H(1,2-diMeIm)	203.1	26.5		1984[h]	
I(1-MeIm)	204.9	26.8	26.5		0.20
I(1,2-diMeIm)	205.4	27.0			0.19

[a] Gerothanassis et al. (1996).
[b] Desbois et al. (1989).
[c] Collman et al. (1976).
[d] Ray et al. (1994).
[e] α-atropisomer.
[f] β-atropisomer.
[g] Two conformers (see text).
[h] Hashimoto et al. (1982).

^{13}C shieldings and, to a lesser extent, ^{18}O isotope effects on the ^{13}C shielding ($^{1}\Delta^{13}C(^{18/16}O)$) indicate a significant variation.

The so-called 'hybrid' models **A**–**C** have two pivalamido pickets (as in the 'picket fence' porphyrin **D**) on each side of an amide handle of variable length linked in a cross-trans configuration. The X-ray structures of the 'hybrid' complexes **A**(1-MeIm) (Ricard et al., 1986) and **B**(1-MeIm) (Tetreau et al., 1994) show that the Fe-C-O unit is both linear and normal to the mean porphyrin plane. All contacts between the terminal oxygen atom and the aliphatic bridging chain are longer than 4 Å and the distance between the porphyrin mean plane and the aliphatic bridging chain is $\geq$8.4 Å (Table 2). For complex **C**(1-MeIm) the X-ray structural data (Tetreau et al., 1994) show a very small bending of the Fe-C-O unit ($\theta = 178.3°$) without tilting (Table 2). Moreover, the iron atom lies almost in the plane formed by the porphyrin nitrogens, but is slightly displaced from the 24-atom core mean plane towards the 1-MeIm ligand.

The 'hybrid' models **A**-**C** have amide links, with the four N-H dipoles turned toward the iron atom. The distance of the secondary amide group of the chain and the CO ligand, N(H)···O(C), is 4.60 Å for model **A**, thus providing an environment of positive polarity for the CO ligand. This polar interaction can be increased via the steric constraint of a short strap. Thus, an increase in the polar interaction might be expected for the **C**(1-MeIm) model, with an N(H) (amide)···O(C) distance of 3.99 Å, compared to that of the model **A**(1-MeIm) and the 'picket fence' model **D** with an N(H) (amide)···O(C) distance of 4.90 Å. This distal polar and electric field effect can be schematically pictured

Table 2. Structural features and rates of CO desorption (k^{-CO}) for CO binding with the heme model compounds of Figure 1

Compound	C-O bond length (Å)	Fe-C bond length (Å)	Fe-M distance[a] (Å)	Shortest NH (amide)···O(CO) (Å)	Fe-C-O angle (°)	$10^3 k^{-CO}$ (s^{-1})
A(1-MeIm)	1.149(6)	1.728(6)	8.43	4.60	180.0[b]	2.7[c]
A(1,2-diMeIm)						110[c]
B(1-MeIm)	1.149(6)	1.752(4)	6.81	4.42	178.9[c]	2.0[c]
B(1,2-diMeIm)						50[c]
C(1-MeIm)	1.149(6)	1.733(4)	6.53	3.99	178.3[c]	8.2[c]
C(1,2-diMeIm)						80[c]
D(1-MeIm)				4.90[d]		7.8[e]
D(1,2-diMeIm)						140[e]
E(1-MeIm)						8.6[f]
E(1,2-diMeIm)[g]	1.148(7)	1.768(7)	5.36	3.76	172.5	55.0[f]
F						6.7[h]
G(1-MeIm)[i]	1.161(8)	1.742(7)	5.57		172.9[j]	50[k]
	1.159(8)	1.748(7)	5.68		175.9[j]	
G(1,2-diMeIm)						
H(1-MeIm)	1.107(13)	1.800(13)	5.86		178.0[l]	
H(1,2-diMeIm)						
I(1-MeIm)						110[m]
I(1,2-diMeIm)						560[m]

[a] Fe-M is the distance between the centroid of the distal cap or strap and the Fe atom; it defines the distal pocket size.
[b] Ricard et al. (1986).
[c] Tetreau et al. (1994).
[d] Estimated from the analogous untethered-picket distances in the crystal structure of **A**(1-MeIm)(CO).
[e] Collman et al. (1976).
[f] Collman et al. (1983a).
[g] β-atropisomer (Kim et al., 1989).
[h] Lavalette et al. (1984).
[i] These are two independent Fe(C_2-Cap)(1-MeIm)(CO) molecules within the asymmetric part of the unit cell.
[j] Kim and Ibers (1991).
[k] Hashimoto et al. (1982).
[l] Slebodnick et al. (1996).
[m] El-Kasmi et al. (1993).

by considering the resonant structures of the FeCO group:

$$\underset{\text{(a)}}{Fe^- - C \equiv O^+} + {}^{\delta+}H \leftrightarrow \underset{\text{(b)}}{Fe = C = O^{\delta+}} - H$$
$$\leftrightarrow \underset{\text{(c)}}{Fe = C = O} + {}^{\delta+}H \qquad (1)$$

A positive potential near the CO carbon atom, as would be the case of the NH dipoles of the amide links, will favor resonance **1(c)** (a decrease in the C-O π-bond order and an increase in the Fe-C π-bond order). According to Buchner and Schenk (1982), $\delta(^{13}C)$ in most transition metal complexes can be expressed in terms of both C-O and Fe-C multiple bonding (Equation 2):

$$\sigma_p^A = \frac{2e^2h^2}{3mc^2\Delta E}\left\langle r_{2p}^{-3}\right\rangle\left[1 - P^{\sigma}_{z_c z_o}P^{\pi}_{y_c y_o} - 3^{1/2}P^{\sigma}_{z_c z^2_{Fe}}P^{\pi}_{y_c yz_{Fe}}\right] \qquad (2)$$

where $P^{\pi}_{y_c yz_{Fe}}$ is the C-Fe(d_{yz}) π-bond order, and $P^{\sigma}_{z_c z^2_{Fe}}$ is the C-Fe(d_z^2) σ-bond order, $P^{\sigma}_{z_c z_o}$ and $P^{\pi}_{y_c y_o}$ are the C-O σ-bond order and π-bond order, respectively. It can be shown that π back-donation will result in a decrease in the C-O π-bond order ($P^{\pi}_{y_c y_o}$) and an increase in the Fe-C π-bond order ($P^{\pi}_{y_c yz_{Fe}}$). Since the σ-bond orders $P^{\sigma}_{z_c z_o}$ and $P^{\sigma}_{z_c z^2_{Fe}}$ are negative, this will result in a decrease in the $-P^{\sigma}_{z_c z_o}P^{\pi}_{y_c y_o}$ term and an increase in the $-P^{\sigma}_{z_c z^2_{Fe}}P^{\pi}_{y_c yz_{Fe}}$ term. If there is significant π bonding between the metal and the carbonyl ligand, the increase will be larger than the decrease, and there

will be a deshielding contribution in Equation 2. This is in agreement with the experimental data of Table 1.

The ^{18}O isotope effects on the ^{13}C shielding of the complexes **A**, **B** and **C** are very similar, 2.6–2.7 Hz (26–27 ppb), and are smaller compared to the values (∼38 ppb) measured in a series of metal carbonyls (Darensbourg and Baldwin, 1979). As expected, upon substitution with a heavier isotope (^{18}O) the ^{13}C NMR signal shifts towards lower frequencies (higher shielding). The X-ray structures of the complexes **A** (Ricard et al., 1986), **B** and **C** (Tetreau et al., 1994) show identical, within experimental error, C-O bond lengths (Table 2).

The ^{13}C NMR spectrum of the so-called 'hanging imidazole' model **F**, which has two NH dipoles turned toward the Fe-C-O unit, indicates the existence of two distinct resonances of ^{13}CO bound to iron with differences between the two magnetic environments (δ = 203.9 and 204.4 ppm). These resonances, with relative population ∼2:1, may be attributed to two forms of the model compound with two orientations of the axial imidazole which differ from each other by 180° (Kalodimos et al., 1997). The $^1J_{^{57}Fe-^{13}C}$ values of both conformers are very similar to those observed for the other amide handle bearing heme model compounds of Table 1.

For the **G**(1-MeIm) complex, in which a benzene cap is attached by carboxylate links and a pair of methylene groups to the four hydroxyl groups of tetrakis(*o*-hydroxylphenyl)porphyrin, the refined X-ray crystal structure shows the presence of two crystallographically independent porphyrin molecules (Kim and Ibers, 1991). The Fe-C-O groups are distorted from linearity (172.9° and 175.9°, Table 2), being tilted off the axis normal to the porphyrin (off-axis displacement for the carbon atoms being 0.17 and 0.12 Å, respectively). These distortions result from short non-bonding interactions between the cap and the CO ligand. The cap is no longer parallel to the porphyrin plane and the porphyrin distortion is very small, presumably because of the constraint of the cap. Only a single ^{13}C isotropic resonance is observed for **G**(1-MeIm), which shows that the interconversion rate of the two conformations is, presumably, fast on the NMR time scale. The very significant shielding of the ^{13}C resonance (δ = 202.1 ppm) compared to the other heme models cannot be attributed to the ring current effect of the aromatic cap. The distance between the center of the benzene ring and the CO carbon is 3.93 and 3.96 Å for the two independent molecules in the cell; therefore, the expected ring current shielding should be ≈0.3 ppm. The significantly different $\delta(^{13}C)$ value for **G**(1-MeIm) very probably results from the nature of the linkages from the porphyrin to the benzene cap. In 'C_2-Cap' there are no NH groups to provide positive polarity near the CO group and the lone pairs of the oxygen of the ester groups provide negative polarity (Ray et al., 1994). Therefore, one would expect an increase in the π-bond order and thus a decrease in $\delta(^{13}C)$. Furthermore, the π electron cloud of the benzene ring is expected to inhibit back-donation from the Fe(II) d_π to the CO π^* orbital due to the small distance between the center of the benzene ring and the CO oxygen (∼2.77 and 2.80 Å for the two independent molecules in the cell).

The above arguments are supported by the fact that when the linker arms are extended by one methylene group, as in **H**(1-MeIm), the shielding decreases (δ = 203.0 ppm) owing to attenuation of the benzene cap interaction. Interestingly, the X-ray structure of Fe(C_3-Cap)(1-MeIm)(CO) indicates an untwisting of the cap which, in combination with the reorientation of the arms, causes a vertical expansion of the cap by 2.36 Å (∼5.86 Å above the mean porphyrin plane) to accommodate CO, from 3.5 Å in H_2(C_3-Cap) (Slebodnick et al., 1996).

For the 'strapped' model **I**, no X-ray structure is available. For ^{13}CO there is a significant increase in the asymmetry of the shielding tensor in the solid ($\eta \sim 0.20$) relative to the complexes of **A**, **B** and **C** (η varies between 0.00 and 0.07), which suggests that there may be increased bending of the Fe-C-O unit in this complex (Gerothanassis et al., 1996). It is interesting to note that this sample also has a significantly higher rate of CO desorption (k^{-CO}) than the other model compounds in this study (Table 2), which results in extensive broadening of both Fe-^{13}CO and ^{13}CO resonances at room temperature. The most likely reason for any increased bending would be strong central steric interactions with the distal protecting chain. Contrary to expectation, however, no difference in the $^1J_{^{57}Fe-^{13}C}$value is observed. Furthermore, $\delta(^{13}C)$ is consistent with a significant degree in back-bonding despite the absence of a distal amide group. As discussed by Li and Spiro (1988), FeCO bending should strongly decrease back-bonding. The electronic effect of FeCO tilting and porphyrin ruffling are more difficult to predict, but an increase in back-bonding is not an obvious result. As discussed in detail by Ray et al. (1994), back-bonding is also influenced by variations in the electron-donating tendency of the substituents of the porphyrin ring. Thus, complexes based on

substituted tetraaryl porphyrins are generally found lower on the back-bonding correlation than adducts based on C_β-alkyl-substituted porphyrins. The alkyl substituents are electron donating and enhance back-donation, while the phenyl substituents are electron withdrawing and decrease back-donation.

Steric effects of proximal imidazole

The introduction of a methyl group in the 2-position of the axial imidazole increases the rate of carbon monoxide dissociation by a factor of 5–40 (Table 2) and the CO affinities are decreased by a factor of 20–100. The steric bulk, therefore, of the axial ligand provides model compounds of the so-called tense ('T') state of hemoproteins. Unfortunately, thus far there has only been one single-crystal X-ray structure determination on such a complex. Kim et al. (1989) have reported the X-ray crystal structure of the β-atropisomer of **E**(1,2-diMeIm) (in which the fourth picket group is in the 'down' position). The Fe-C-O bond angle was found to be 172.5° (Table 2) and the off-axis displacements of the C and O atoms are 0.18 and 0.38 Å, respectively. The modest distortion of the Fe-C-O unit is accompanied by considerable ruffling of the porphyrin periphery and significant shifting of the benzene 'cap' away from the bound CO ligand. Moreover, the Fe atom is only 0.001 Å out of the 24-atom least-squares plane towards the CO ligand and the Fe-C bond length appears to be longer compared with the 1-MeIm adducts. During our synthesis of **E**(1,2-diMeIm), we observed that both α- and β-atropisomers exist in solution, with relative integrals 3 to 2 (Figure 2). Although the X-ray crystal structure of the β-atropisomer of the **E**(1,2-diMeIm) adduct shows very similar FeCO geometries to that of the **G**(1-MeIm) model, involving a small amount of bending and tilting, their ^{13}C shieldings are very different. These contrasting patterns can be attributed to the different polar interactions of the bound CO in the two adducts. In the 'PocPiv' adduct, the oxygen atom is in close contact with one of the amide NH groups. This positive polar interaction increases back-bonding.

Comparison of the results for the 1-MeIm and 1,2-diMeIm complexes of the porphyrins (**A**–**I**) surprisingly shows no significant differences in the $^1J_{^{57}Fe-^{13}C}$ values despite higher rates of CO desorption being observed for the 1,2-diMeIm adducts and the expected lengthening of the Fe-C bond length. In conclusion, the ^{57}Fe-^{13}CO couplings, contrary to earlier claims (La Mar et al., 1978), are not accurate monitors of the multiple mechanisms by which steric and electronic interactions are released in superstructured heme model compounds and hemoproteins. Interestingly, $^1J_{^{57}Fe-^{13}C}$ of ^{13}C-labelled isocyanides bound to myoglobin and synthetic porphyrins were found to be susceptible neither to variation of the alkyl rest R at the RNC ligand nor to the presence of the globin (Morishima et al., 1979). In contrast, ^{13}C shows a consistent deshielding of the 1,2-diMeIm adducts which varies between 0.1 and 0.6 ppm (Table 1). This is consistent with the expected strengthening of the Fe-C bond when the axial imidazole bond is weakened by the proximal steric hindrance.

Correlations between $\delta(^{13}C)$, $^1\Delta^{13}C(^{18/16}O)$ and ν(C-O) – Comparison with hemoproteins

Several workers (Paul et al., 1985; Li and Spiro, 1988; Oldfield et al., 1991; Ray et al., 1994) have noted a negative correlation between $\delta(^{13}C)$ versus ν(C-O) and ν(C-O) versus ν(Fe-C) for a variety of metal carbonyl adducts and have discussed this effect in terms of back-bonding in the FeCO unit. When $\delta(^{13}C)$ is plotted against ν(C-O) for the CO adducts of the superstructured heme model compounds of Table 1, a linear correlation is observed, corresponding to the solid line drawn in Figure 3. The relation can be expressed as

$$\delta(^{13}\mathrm{C},\ \mathrm{ppm}) = -0.0721\,\nu(\mathrm{C\text{-}O},\ \mathrm{cm}^{-1}) + 346.2$$

with a correlation coefficient of 0.967.

From the above, it is evident that strong back-bonding decreases the C-O π-bond order and increases the deshielding for ^{13}C while simultaneously decreasing ν(C-O). If this 'back-bonding' model, used previously by Li and Spiro (1988), is correct, then one would predict a monotonic relation between $^1\Delta^{13}C(^{18/16}O)$, which is one monitor of the C-O bond length (Jameson and Osten, 1985), and both $\delta(^{13}C)$ and ν(C-O). Figures 4 and 5 show linear relationships between $^1\Delta^{13}C(^{18/16}O)$ as a function of $\delta(^{13}C)$ and ν(C-O), the actual values used being shown in Table 1. We now have the following two additional relationships for heme model compounds:

$$^1\Delta^{13}C(^{18/16}\mathrm{O},\ \mathrm{ppb}) = -1.8918\delta(^{13}\mathrm{C},\ \mathrm{ppm}) + 415.1$$

with a correlation coefficient of 0.874 and

$$^1\Delta^{13}C(^{18/16}\mathrm{O},\ \mathrm{ppb}) = 0.1312\nu(\mathrm{C\text{-}O},\ \mathrm{cm}^{-1}) - 229.5$$

with a correlation coefficient of 0.832.

When the ^{18}O isotope shifts ($^1\Delta^{13}C(^{18/16}O)$, ppb) are plotted against crystallographic CO bond lengths

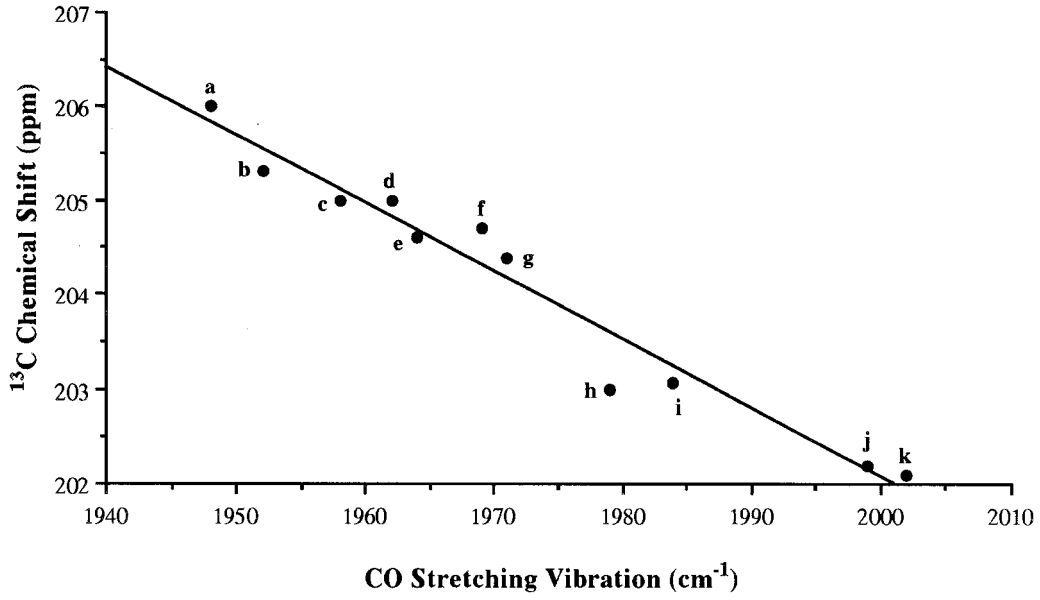

Figure 3. Plot showing the relation between ^{13}C NMR isotropic chemical shift ($\delta(^{13}C)$, ppm) and infrared CO vibrational stretching frequency (ν(C-O), cm^{-1}) for heme model compounds. Data points are as follows: a, **C**(1-MeIm); b, **B**(1-MeIm); c, **A**(1-MeIm); d, **D**(1,2-diMeIm); e, **E**(1-MeIm); f, **D**(1-MeIm); g, **F**; h, **H**(1-MeIm); i, **H**(1,2-diMeIm); j, **G**(1,2-diMeIm); k, **G**(1-MeIm).

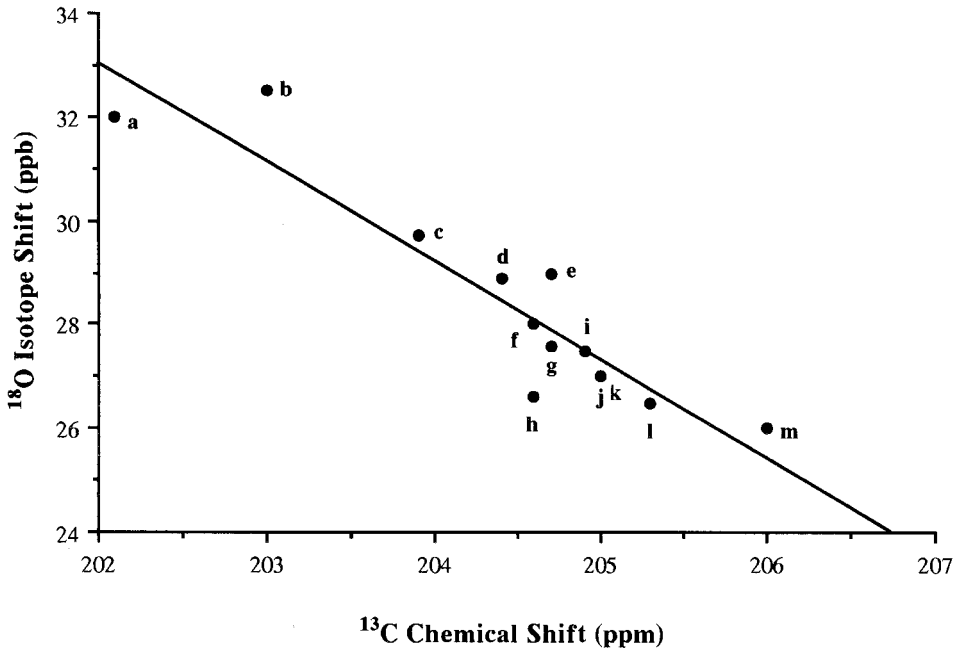

Figure 4. Plot showing the relation between ^{18}O isotope effect on ^{13}C shielding ($^{1}\Delta^{13}C$ ($^{18/16}$O), ppb) and ^{13}C isotropic chemical shifts ($\delta(^{13}C)$, ppm) for heme model compounds. Data points are as follows: a, **G**(1-MeIm); b, **H**(1-MeIm); c and d, **F** (two conformers, see text); e, **D**(1-MeIm); f, **E**(1-MeIm); g, **E**(1,2-diMeIm) (β-atropisomer); h, **E**(1,2-diMeIm) (α-atropisomer); i, **I**(1-MeIm); j, **D**(1,2-diMeIm); k, **A**(1,2-diMeIm); l, **B**(1-MeIm); m, **C**(1-MeIm).

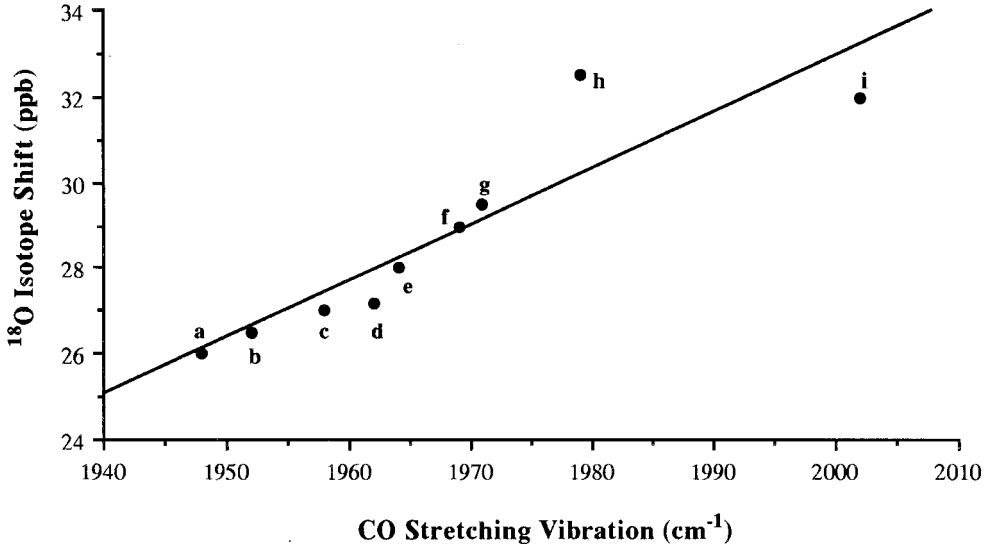

Figure 5. Plot showing the relation between ^{18}O isotope effect on ^{13}C shieldings ($^{1}\Delta^{13}$C ($^{18/16}$O), ppb) and infrared CO vibrational stretching frequency (ν(C-O), cm^{-1}) for heme model compounds. Data points are as follows: a, **C**(1-MeIm); b, **B**(1-MeIm); c, **A**(1-MeIm); d, **D**(1,2-diMeIm); e, **E**(1-MeIm); f, **D**(1-MeIm); g, **F**; h, **H**(1-MeIm); i, **G**(1-MeIm).

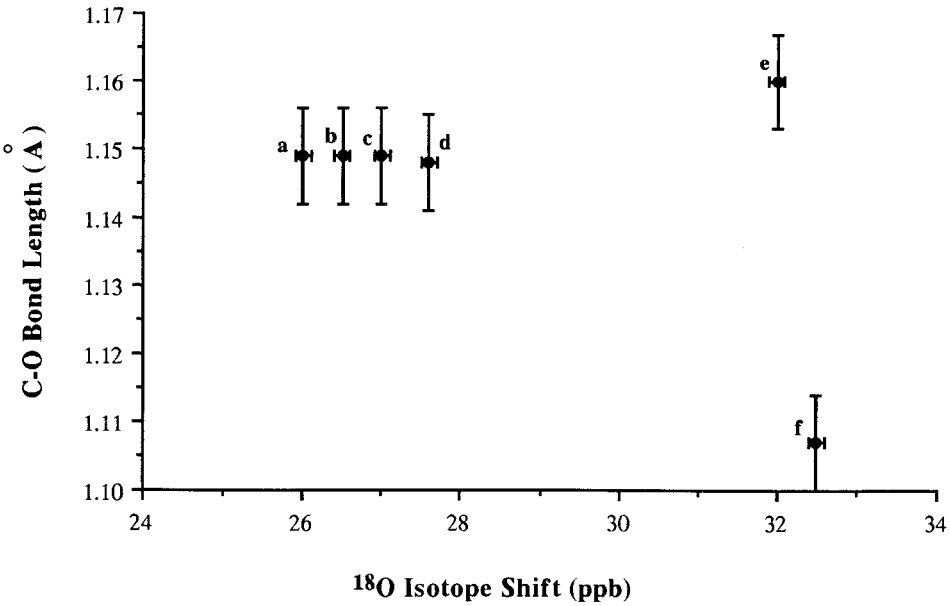

Figure 6. Plot of crystallographic r(C-O) (Å) versus $^{1}\Delta^{13}$C($^{18/16}$O) (ppb) of the ^{13}CO complexes for heme model compounds. The vertical bars denote the accuracy of the X-ray structures while the horizontal ones denote the accuracy of the NMR measurements. Data points are as follows: a, **C**(1-MeIm); b, **B**(1-MeIm); c, **A**(1-MeIm); d, **E**(1,2-diMeIm) (β-atropisomer); e, **G**(1-MeIm); f, **H**(1-MeIm). For **G** an average C-O bond distance of 1.160 Å was used.

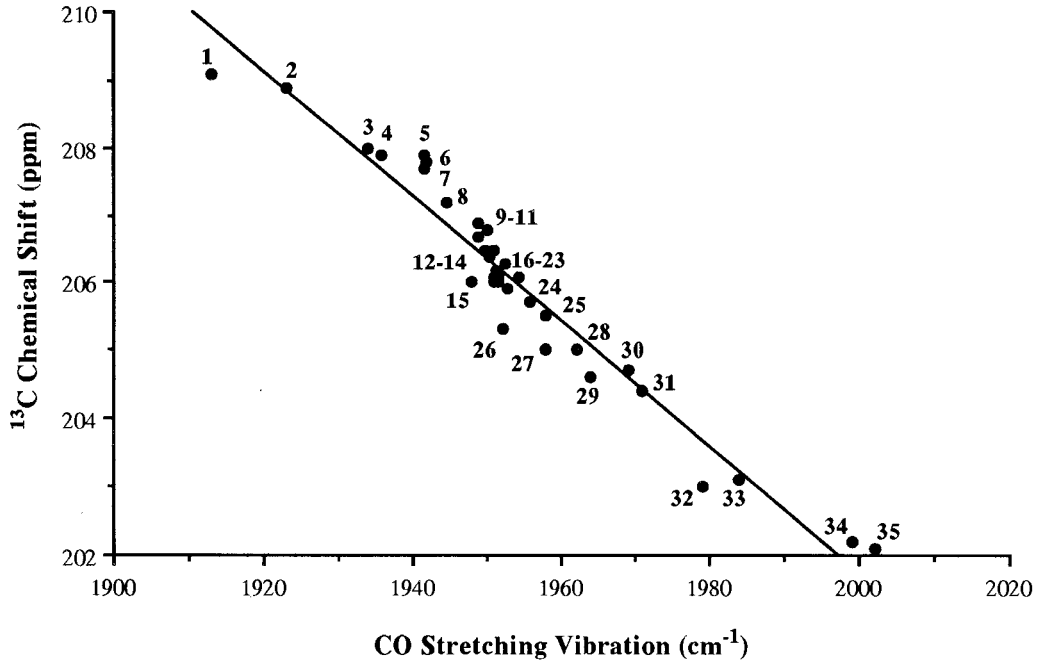

Figure 7. Plot showing the relation between ^{13}C isotropic chemical shift ($\delta(^{13}C)$, ppm) and infrared CO vibrational stretching frequency (ν(C-O), cm^{-1}) for heme model compounds and a variety of hemoproteins (Potter et al., 1990; Park et al., 1991). Data points are as follows: 1, horseradish peroxidase isoenzyme C, pD = 6.4; 2, horseradish peroxidase isoenzyme A, pD = 6.8; 3, rabbit I Hb, α subunit; 4, rabbit II Hb, α subunit; 5, sperm whale Mb; 6, equine Mb; 7, bovine Mb; 8, opossum Hb, α subunit; 9, guinea pig Hb, α subunit; 10, bovine Hb, α subunit; 11, horse Hb, α subunit; 12, HbZn, α subunit; 13, rabbit Hb, α subunit; 14, jackrabbit Hb, α subunit; 15, **C**(1-MeIm); 16, bovine Hb, β subunit; 17, guinea pig Hb, β subunit; 18, rat Hb; 19, β-chain from HbA, pH = 7.2; 20, opossum Hb, β subunit; 21, HbA, β subunit, pH = 7.4; 22, rabbit I Hb, β subunit; 23, HbA, α subunit, pH = 4.6; 24, HbA, β subunit, pH = 4.6; 25, HbZn, β subunit, pH = 7.7; 26, **B**(1-MeIm); 27, **A**(1-MeIm); 28, **D**(1,2-diMeIm); 29, **E**(1-MeIm); 30, **D**(1-MeIm); 31, **F**; 32, **H**(1-MeIm); 33, **H**(1,2-diMeIm); 34, **G**(1,2-diMeIm); 35, **G**(1-MeIm).

(r(C-O), Å), then, paradoxically, no correlation is observed (Figure 6). It is also particularly surprising that the C-O bond length of the Fe(C_3-Cap)(1-MeIm)(CO) model is shorter (∼1.107 Å) compared to other model compounds of Table 2 (average distance ∼1.150 Å) while that of the Fe(C_2-Cap)(1-MeIm)(CO) model is longer (1.161 and 1.158 Å). Thus, it appears that the lack of correlation between $^1\Delta^{13}C(^{18/16}O)$ and crystallographic CO bond lengths reflects significant uncertainties in the X-ray determination of the carbon and oxygen position (ESDs of ca. $\gg$0.01 Å).

The above $\delta(^{13}C)$ versus ν(C-O) correlations appear significant in view of the large number of model compounds involved. This suggests an alternative way for comparing the trends in ligand binding in different heme model families with those of heme proteins. When several HbCO species at different pH values and three different MbCO species are included in the $\delta(^{13}C)$ versus ν(C-O) correlation, this remains essentially linear (Figure 7) and can be expressed as

$$\delta(^{13}\text{C, ppm}) = -0.0921\nu(\text{C-O, cm}^{-1}) + 386.0$$

with a correlation coefficient of 0.955. The use of weighted-average ν(C-O) is required since hemoprotein subunits exhibit absorbance at more than one frequency and yet have only one NMR resonance (Potter et al., 1990). This can be explained in terms of a rate of interconversion among conformers that is greater than the NMR time scale (∼10^{-4} s). The ^{13}C resonances of heme proteins cover a 3.5 ppm range and the computed weighted-average vibrational frequencies vary by 45 cm^{-1}. This range is extended to 7.0 ppm when the ^{13}C shieldings of the heme models are included. This demonstrates that both heme models and heme proteins are homogeneous from the structural and electronic viewpoint.

Horseradish peroxidase (HRP) exhibits the most deshielded ^{13}CO resonances observed in hemoproteins and model compounds (points 1 and 2 in Figure 7). It has been suggested that the negative charge on the terminal Fe-CO oxygen atom increases, in comparison with HbCO, since the anionic proximal imidazolate ligand accelerates the polarization of the distal

CO ligand. In addition, the strong hydrogen bond of the bound CO with the distal histidine residue enhances back-donation from the Fe (Tokita and Nakatsuji, 1997). MbCO and HbCO show greater back-bonding than the site-directed mutants with non-polar distal E7 residues, e.g. glycine, valine or phenylalanine (Morikis et al., 1989), because the distal histidine, or glutamine in elephant Mb (Lin et al., 1990), provides a positive polar interaction for the bound CO.

Our results, therefore, favor the conclusion of Oldfield et al. (1991), Park et al. (1991) and Ray et al. (1994) that the main mechanism determining the change in $\delta(^{13}C)$ and ν(C-O) of the CO coordinated to heme proteins and their models is of dipolar and electrostatic nature with distal residues.

Conclusions

We have presented ^{57}Fe-^{13}C(O) coupling constants, ^{13}C shieldings and ^{18}O isotope effects on ^{13}C shieldings of several carbon monoxide (99.7% ^{13}C and 11.8% ^{18}O enriched) hemoprotein models with varying polar and steric effects of the distal organic superstructure and constraints of the proximal side. Polar interactions in the binding pocket and modulation of Fe→CO back-donation appear to have a very significant effect on $\delta(^{13}C)$, moderate effect on $^{1}\Delta^{13}C(^{18/16}O)$ and little direct effect on $^{1}J_{^{57}Fe-^{13}C}$couplings. The ^{13}C shieldings of heme models cover a 4.0 ppm range which is extended to 7.0 ppm when several HbCO and MbCO species at different pH values are included. The excellent linear $\delta(^{13}C)$ versus ν(C-O) relationship proves that both heme models and heme proteins are homogeneous from the structural and electronic viewpoint. The extensive $\delta(^{13}C)$ and ν(C-O) data on heme proteins and synthetic models suggest that there is little direct correlation between $\delta(^{13}C)$ and Fe-C-O geometry. The major factor governing both $\delta(^{13}C)$ and ν(C-O) appears to be the electrostatic field surrounding the bound ligand and not steric hindrance. Positive polar interactions of bound CO with distal residues decrease the C-O π-bond order, resulting in an increase in $\delta(^{13}C)$ and a decrease in ν(C-O). Elimination of polar interactions reverses the above effects.

Though much remains to be done to understand in greater detail the implications of the correlations observed, the biomimetic chemical approach to heme protein systems provides a convenient means for comparing model families with each other and with the heme proteins. It is therefore possible to estimate the relative importance of electronic and stereochemical parameters which contribute to the overall activity of heme proteins.

Acknowledgements

This research was supported by the Greek General Secretariat of Research and Technology, a Franco-Hellenique Collaborative Research Grant, FEBS (summer term fellowship to C.G.K.) and the Greek Scholarship Foundation (Ph.D. research fellowship to C.G.K.).

References

Almog, J., Baldwin, J.E. and Huff, J.R. (1975) *J. Am. Chem. Soc.*, **97**, 227–228.

Buchner, W. and Schenk, W.A. (1982) *J. Magn. Reson.*, **48**, 148–151.

Collman, J.P., Brauman, J.I., Halbert, T.R. and Suslick, K.S. (1976) *Proc. Natl. Acad. Sci. USA*, **73**, 3333–3337.

Collman, J.P., Brauman, J.I., Collins, T.J., Iverson, B.L., Lang, G., Pettman, R.B., Sessler, J.L. and Walters, M.A. (1983a) *J. Am. Chem. Soc.*, **105**, 3038–3052.

Collman, J.P., Brauman, J.I., Iverson, B.L., Sessler, J.L., Morris, R.M. and Gibson, Q.H. (1983b) *J. Am. Chem. Soc.*, **105**, 3052–3064.

Darensbourg, D.J. and Baldwin, B.J. (1979) *J. Am. Chem. Soc.*, **101**, 6447–6449.

Desbois, A., Momenteau, M. and Lutz, M. (1989) *Inorg. Chem.*, **28**, 825–835.

Dickerson, R.E. and Geis, I. (1983) *Hemoglobin: Structure, Function, Evolution and Pathology*, Benjamin/Cummings, Menlo Park, CA.

El-Kasmi, D., Tetreau, C., Lavalette, D. and Momenteau, M. (1993) *J. Chem. Soc., Perkin Trans. 2*, 1799–1803.

Gerothanassis, I.P. (1994) *Prog. NMR Spectrosc.*, **26**, 239–292.

Gerothanassis, I.P., Momenteau, M., Barrie, P.J., Kalodimos, C.G. and Hawkes, G.E. (1996) *Inorg. Chem.*, **35**, 2674–2679.

Hashimoto, T., Dyer, R.L., Crossley, M.J., Baldwin, J.E. and Basolo, F. (1982) *J. Am. Chem. Soc.*, **104**, 2101–2109.

Jameson, C.J. and Osten, H.-J. (1985) *J. Am. Chem. Soc.*, **107**, 4158–4161.

Jameson, G.B. and Ibers, J.A. (1994) In *Bioinorganic Chemistry* (Eds., Bertini, I., Gray, H.B., Lippard, S. and Valentine, J.S.), University Science Books, Mill Valley, CA, pp. 167–252.

Kalodimos, C.G., Gerothanassis, I.P., Troganis, A. and Momenteau, M. (1997) In *Spectroscopy of Biological Molecules: Modern Trends* (Eds., Carmona, P., Navarro, R. and Hernanz, A.), Kluwer, Dordrecht, pp. 77–78.

Kim, K., Fettinger, J., Sessler, J.L., Cyr, M., Hugdahl, J., Collman, J.P. and Ibers, J.A. (1989) *J. Am. Chem. Soc.*, **111**, 403–405.

Kim, K. and Ibers, J.A. (1991) *J. Am. Chem. Soc.*, **113**, 6077–6081.

Kushkuley, B. and Stavrov, S.S. (1997) *Biophys. J.*, **72**, 899–912.

La Mar, G.N., Viscio, D.B., Budd, D.L. and Gersonde, K. (1978) *Biochem. Biophys. Res. Commun.*, **82**, 19–23.

Lavalette, D., Tetreau, C., Mispelter, J., Momenteau, M. and Lhoste, J.-M. (1984) *Eur. J. Biochem.*, **145**, 555–565.
Li, X.-Y. and Spiro, T.G. (1988) *J. Am. Chem. Soc.*, **110**, 6024–6033.
Lin, S.-H., Yu, N.-T., Tame, J., Shih, D., Renaud, J.-P., Pagnier, J. and Nagai, K. (1990) *Biochemistry*, **29**, 5562–5566.
Momenteau, M. (1986) *Pure Appl. Chem.*, **58**, 1493–1502.
Momenteau, M., Loock, B., Tetreau, C., Lavalette, D., Croisy, A., Schaeffer, C., Huel, C. and Lhoste, J.-M. (1987) *J. Chem. Soc., Perkin Trans. 2*, 249–257.
Momenteau, M. and Reed, C.A. (1994) *Chem. Rev.*, **94**, 659–698.
Morikis, D., Champion, P.M., Springer, B.A. and Sligar, S.G. (1989) *Biochemistry*, **28**, 4791–4800.
Morishima, I., Hayashi, T. and Yonezawa, T. (1979) *J. Chem. Soc., Chem. Commun.*, 483–485.
Oldfield, E., Guo, K., Augspurger, J.D. and Dykstra, C.E. (1991) *J. Am. Chem. Soc.*, **113**, 7537–7541.
Park, K.D., Guo, K., Adebodun, F., Chiu, M.L., Sligar, S.G. and Oldfield, E. (1991) *Biochemistry*, **30**, 2333–2347.
Paul, J., Smith, M.L. and Paul, K.-G. (1985) *Biochim. Biophys. Acta*, **832**, 257–264.
Perutz, M.F., Fermi, G., Luisi, B., Shaanan, B. and Liddington, R.C. (1987) *Acc. Chem. Res.*, **20**, 309–321.
Potter, W.T., Hazzard, J.H., Choc, M.J., Tucker, M.P. and Caughey, W.S. (1990) *Biochemistry*, **29**, 6283–6295.
Ray, G.B., Li, X.-Y., Ibers, J.A., Sessler, J.L. and Spiro, T.G. (1994) *J. Am. Chem. Soc.*, **116**, 162–176.
Ricard, L., Weiss, R. and Momenteau, M. (1986) *J. Chem. Soc., Chem. Commun.*, 818–820.
Slebodnick, C., Fettinger, J.C., Peterson, H.B. and Ibers, J.A. (1996) *J. Am. Chem. Soc.*, **118**, 3216–3224.
Springer, B.A., Sligar, S.G., Olson, J.S. and Phillips Jr., G.N. (1994) *Chem. Rev.*, **94**, 699–714.
Stryer, L. (1988) *Biochemistry*, Freeman, San Francisco, CA.
Tetreau, C., Lavalette, D., Momenteau, M., Fischer, J. and Weiss, R. (1994) *J. Am. Chem. Soc.*, **116**, 11840–11848.
Tokita, Y. and Nakatsuji, H. (1997) *J. Chem. Phys. B*, **101**, 3281–3289.
Wasylishen, R.E., Friedrich, J.O., Mooibroek, S. and Macdonald, J.B. (1985) *J. Chem. Phys.*, **83**, 548–551.